CHAPTER 124

TURBULENCE IN HURRICANE-GENERATED COASTAL CURRENTS

By Stephen P Murray
Coastal Studies Institute
Louisiana State University
Baton Rouge, Louisiana 70803

ABSTRACT

Wind and current meter records taken during the passage of a hurricane were subjected to time series analysis Filtering techniques isolated the speed fluctuations in the 10-60 CPH frequency band These turbulent fluctuations proved to follow the Gaussian distribution for both wind and current With the passage of the storm front the turbulence intensity of the wind actually decreased, while, on the other hand, the turbulence intensity of the current rose to extremely large values, even exceeding 27 percent of the mean flow speed

Three phases of the storm were examined separately, and the energy density of the wind varied with the -1 power of the frequency in all phases With respect to the energy density of the current, a -1 power dependency on the frequency was approximated by the first two phases, whereas in the third phase, which was the most intense, the energy density varied approximately as the -0 5 power of the frequency The characteristics of the spectra indicate that there is little direct transfer of energy from the wind to the current in the frequency range studied Energy is passing into the 10-60 CPH band of the current from still lower frequencies

INTRODUCTION

Hurricane-generated coastal currents can attain enormous magnitude and are instrumental in inflicting material damage and producing changes in coastal topographies which result in great monetary losses The undermining of piers and jetties and the destruction of sea buoys and other navigation aids illustrate this point clearly However, owing to scarcity of data, the characteristics of currents produced by hurricane winds remain essentially unknown

Hurricane Camille traversed the Gulf of Mexico on a northwesterly track during the period August 15-17, 1969, and made its landfall at Gulfport, Mississippi (Fig 1) During this time the Coastal Studies Institute was conducting a shallow-water oceanographic measuring program at its field facility on the Eglin Air Force Base Santa Rosa Island Testing Grounds This locality, 160 km to the east of the hurricane landfall, was subjected to severe winds, high waves, and storm surge Of several current meters installed on the nearshore bottom prior to the storm, one placed at the depth of 6 3 meters beyond the outer bar provided an excellent time series record of the current during the storm

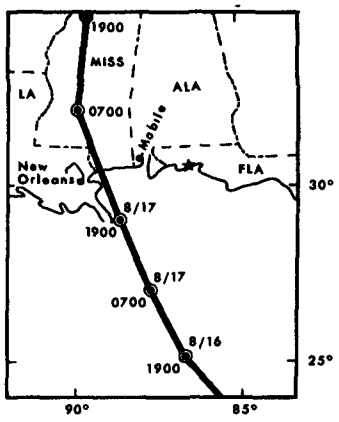

Fig 1 Track of the eye of Hurricane Camille, August 16 and 17, 1969

An anemometer mounted 12 meters above the water level on the adjacent beach operated concurrently

The correlative aspects, especially in respect to the coastal circulation, of mean speeds and directions of both the current record and the wind record were discussed in Murray (1970) The purpose of the present paper is to discuss the properties of the turbulence associated with the hurricane winds and currents, with special reference to the turbulence, the energy density spectra, and cross spectra and coherence between these two signals

INSTRUMENTATION

The current sensor was a Marine Advisers bottom-mounted Q-16 bidirectional integrating meter which utilizes a ducted impeller assembly of small mass with a threshold speed rated at 0 08 knots The duct is fitted with a vane that is long relative to the wave's orbital diameter, thus the vane holds the meter with its axis aligned with the steady current A magnetic compass assembly within the instrument determines magnetic north, the orientation of the vane then determines the current direction

The current speed sensor contains two reed switches that are activated by magnets on the blades of the impeller The reed switches are mounted so that they open and close at slightly different times, which allows the electronic circuitry to determine the direction of rotation of the impeller If the impeller is turning in the direction of the net current, a differential amplifier integrator integrates the pulses in the positive direction, if the impeller turns in the opposite direction, the amplifier integrates in the negative direction There is then produced at the output of the amplifier a DC voltage proportional to the net current through the speed sensor This voltage represents a time average over a time interval determined by the fixed time constant τ of the proper RC circuit Given a step function increase in the current speed up to a value V_o, the output speed V lags the true speed V_o according to

$$V = V_o \ (1 - e^{-t/\tau})$$

Thus one time constant is the time required for the output speed to reach $(1 - e^{-1}) \sim 63$ percent of the true speed In the present case, the time constant was fixed at 6 2 seconds

Instruments with time constants function as filters which smooth, lag, and damp cycles in the output as a function of the frequency f The frequency response R(f) (the ratio of output amplitude to true amplitude)

of a "time constant" filter is (Holloway, 1958)

$$R(f) = (1 + 4\pi^2\tau^2f^2)^{-1/2}, \quad (1)$$

and the phase lag is

$$\phi = \tan^{-1}(-2\pi\tau f) \quad (2)$$

The frequency response function with τ = 6 2 seconds, together with the phase lag, is shown in Figure 2 It is seen from the figure that there is at least 88 percent response for frequencies below 50 CPH Since the frequency range of surface waves during the hurricane was between 450 and 720 CPH (5-8 second periods), the sensor response to waves was held to only 12-20 percent (frequency response at the output)

The Q-16 current meter assembly was situated on the bottom 360 meters seaward of the shoreline in 6 3 meters of water The speed sensor duct was 1 5 meters above the sandy bottom

The anemometer was a Science Associates No 162 General Purpose Wind Recording System The response characteristics of this particular instrument are not precisely known, but the sensitivity of this standard type three-cup anemometer has been well studied in the past Fergusson (1935) measured 2 30, 0 60, and 0 33 seconds for a standard three-cup anemometer to accelerate from zero speed up to 5, 20, and 35 m/sec respectively It is conservative to say that our anemometer of this type has a full response for cycles with a period of 10 seconds or 360 CPH

ANALYSIS TECHNIQUES

Strip chart recorders were used which had response times of 0 8 seconds for the current recorder and 0 5 seconds for the wind recorder The factors exerting ultimate control over the frequency response, however, were the recorder chart speeds--4 inches per hour for the current recorder and 3 inches per hour for the wind recorder The trace width allowed only frequencies less than 50 CPH to be absolutely discriminated on both strip charts at these chart speeds

The strip chart records were digitized on a Calma Model 303 Digitizer, which transfers graphical analog data to digital magnetic tapes by visually tracing the graphic data Visual tracing in this case represents a smoothing filter which insures that no frequencies higher than about 60 CPH are transferred to the magnetic tape The digitizer was set to record incrementally the coordinates of 100 points per inch of strip chart data Owing to the two different chart speeds, this procedure produces a data density discrepancy which is eliminated by an interpolation option in the Calma software programs The selected interpolation procedure yielded 100 data points per hour of record

Thirteen hours of data between 0400 and 1700 hours August 17 (2600 data points) were placed on the magnetic tape for analysis This interpolated version of the original observations was plotted by computer and

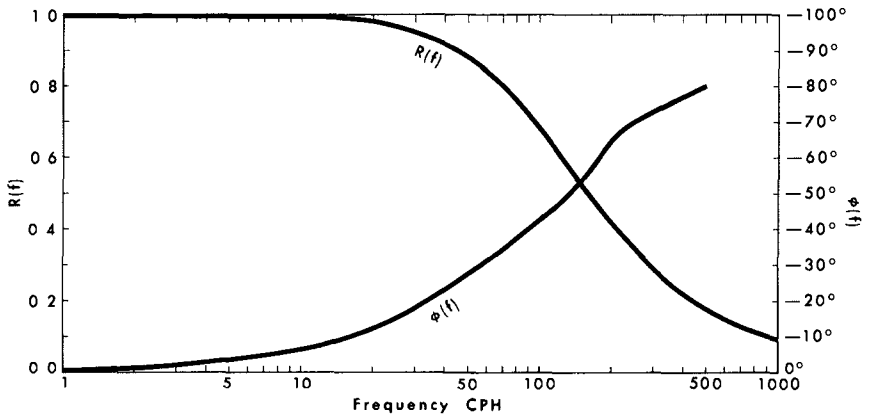

Fig 2 Frequency response and phase lag for a "time constant" filter with τ = 6 2 seconds

is shown as Figure 3 Inspection of the figure shows that (a) the initial one third of this record (phase I) represents a pre-storm front phase, (b) the middle one third (II) represents an accelerative phase during which both the wind and current speeds increased rapidly after the storm front passage, and (c) the final third is a relatively steady phase (III) for both mean wind and mean current speeds

The data length and time increment selects the highest and lowest frequencies which are present in the data For N observations taken at ΔT seconds apart this spectral band is approximately

$$\frac{1}{2N\Delta T} < f \leq \frac{1}{2\Delta T}$$

In this study N = 2600, ΔT = 0 005 hours, and the observable frequency band is 0 04 < f < 100 CPH The frequency $1/2\Delta T$ = 100 CPH is known as the Nyquist frequency f_c In spectral analysis all power contained in frequencies higher than f_c is folded back into the spectra below f_c, resulting in aliasing One method of avoiding this problem (Bendat and Piersol, 1966) is to select a Nyquist frequency sufficiently higher than the maximum frequency of interest to insure that there is little power in the frequencies $f > f_c$ From the discussion of the digitizing of the relatively slow chart speeds and the frequency response curve in Figure 2, it is clear that there is little power above f_c = 100 CPH for aliasing

Before spectral analysis of time series data is performed, any trends or very low frequency oscillations must be eliminated from the data, or the resulting spectra may be considerably distorted (Bendat and Piersol, 1966) A smoothing function which is essentially a low

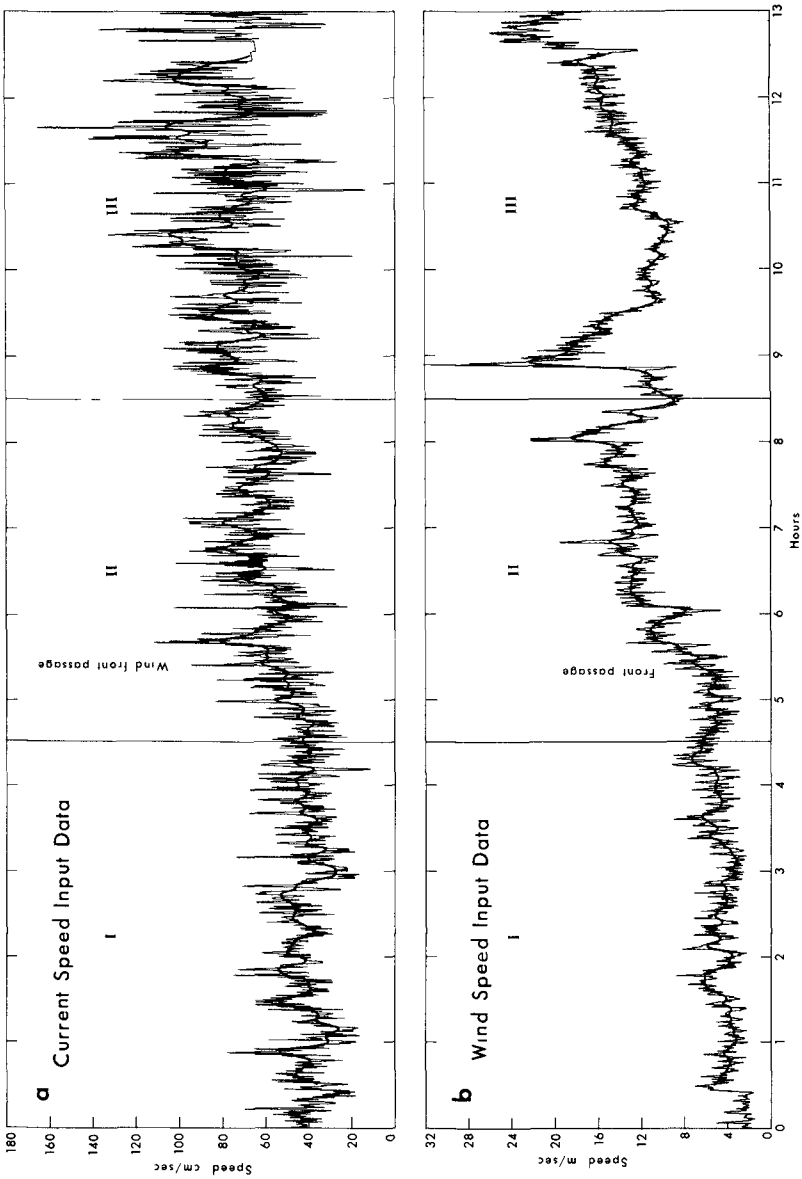

Fig 3 The time series observations of (a) the current and (b) the wind speeds together with the smoothed speeds determined by a 201-point binomial filter The three phases subjected to separate analyses are shown in Roman numerals

pass filter can be used to isolate the trends and low frequency components In Figure 3 the smoothed curve running through the observed data was derived from a 201-point binomial filter whose frequency response $R(f)_{BF201}$ is plotted in Figure 4 using the relation $R(f) = \cos^n(\pi f \Delta T)$ where n is the number of terms in the filter less one This smoothing function passes only 8 percent of the amplitude of frequencies above 10 CPH and completely cuts out those amplitudes with f ≥ 15 CPH

The next step is the subtraction of the smoothed time series from the original time series, which is a high pass filtering technique (Holloway, 1958, Panofsky and Brier, 1963) with a frequency response R'(f) in this case

$$R'(f) = 1 - R(f)_{BF201},$$

also plotted in Figure 4 All frequencies with f ≥ 10 CPH have at least 90 percent of their amplitudes transmitted through the filter, and, again considering the filtering performed in digitizing, the final form of the data is a band pass $10 \lesssim f \lesssim 60$ CPH

Also plotted in Figure 4 for comparison is the response of a high pass filter produced by subtracting a 30-point equally weighted running mean from an original time series This type filter provides a sharper cut with minimal data loss but has distinct disadvantages in that it amplifies and damps certain frequencies, the troughs in the response curve turn maxima into minima and may produce a falsely rippled power spectrum (Holloway, 1958) A preliminary analysis of the present data with a 30-point equally weighted running mean high pass filter did in fact produce pronounced peaks at 30 and 50 CPH which could have been erroneously interpreted as surf beat effects

TURBULENCE

Let us denote the original time series observations of speed by u_o and the smoothed record using the 201 binomial smoothing "function" by U_{BF} The turbulent speed u' may be defined following the conventional theory by

$$u' \equiv u_o - U_{BF}$$

The random nature of u' is indicated by the histograms of u' (both wind and current), which show a good agreement with the corresponding best-fit Gaussian curves (Figure 5)--typical of most turbulence measurements

In Figure 6 the turbulence intensity $(\overline{u'^2})^{1/2}$ and the relative turbulence intensity $(\overline{u'^2})^{1/2}/\bar{U}_{BF}$ are plotted as a function of time The term $(\overline{u'^2})^{1/2}$ was calculated each half hour as the root-mean-square value of the 100 observations in that time interval, whereas the term $\bar{U}_{BF}$ is the average of the corresponding 100 values of U_{BF} in that same time interval The turbulence intensity of the current increased fairly

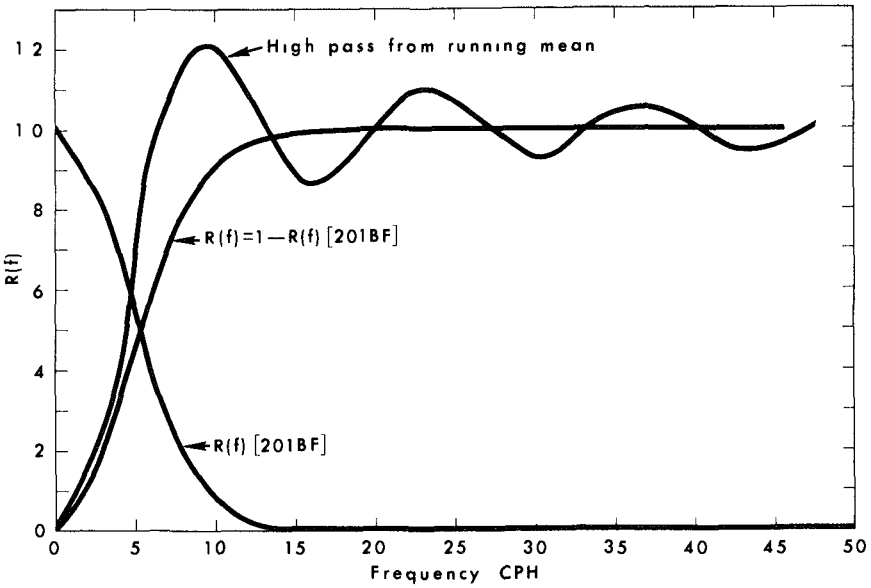

Fig 4 Frequency response curves for the high and low pass filters discussed in the text

regularly as the storm progressed from 8 cm/sec up to 22 cm/sec, while relative to the mean speed it oscillated around a value of about 0 18 cm/sec, even reaching as high as 0 27 cm/sec near the end of the record Many previous studies in both field and laboratory have shown that the turbulence intensity under more normal conditions varies between 0 05 and 0 15 cm/sec of the mean flow speed The turbulence intensity of the wind increased from an initial value of 75 cm/sec up to 150 cm/sec in the seventh hour The relative value stayed at about 0 20 cm/sec until it dropped precipitously with the arrival of the storm front and its high mean speeds at hour 5 3 (see Fig 3b)

It is notable that the turbulence intensity of the wind was decidedly damped after the front passed (excepting the effect of the large gust at 8 9 hours) The current turbulence intensity, on the other hand, inversed after the front passed It is significant that the current direction abruptly shifted (see Murray, 1970) after the wind front passed from westerly to southwesterly and south, reflecting, it is believed, a seaward return flow caused by setup against the coast The increase in current turbulence intensity was probably caused by (a) the large vertical shear inherent within a reversing velocity profile and (b) the effects of large groups of wind-driven waves associated with the suddenly increased mean wind

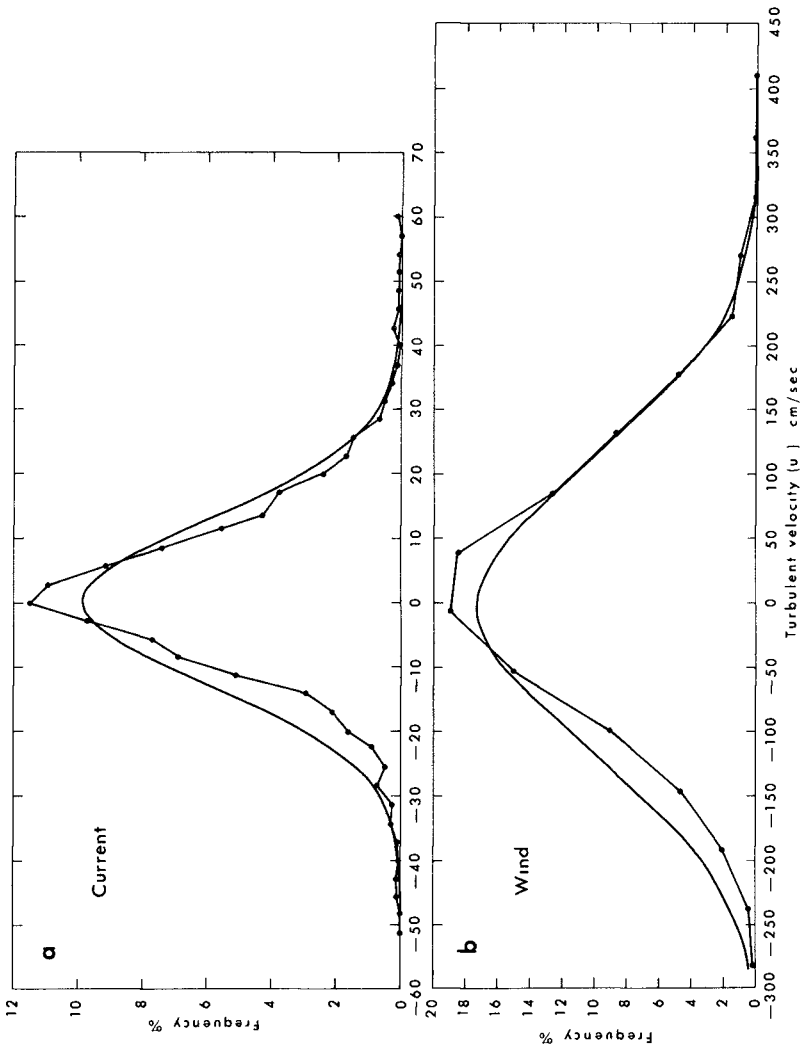

Fig 5 Frequency distributions of (a) the turbulent current speeds and (b) the turbulent wind speed together with the best-fit Gaussian curves

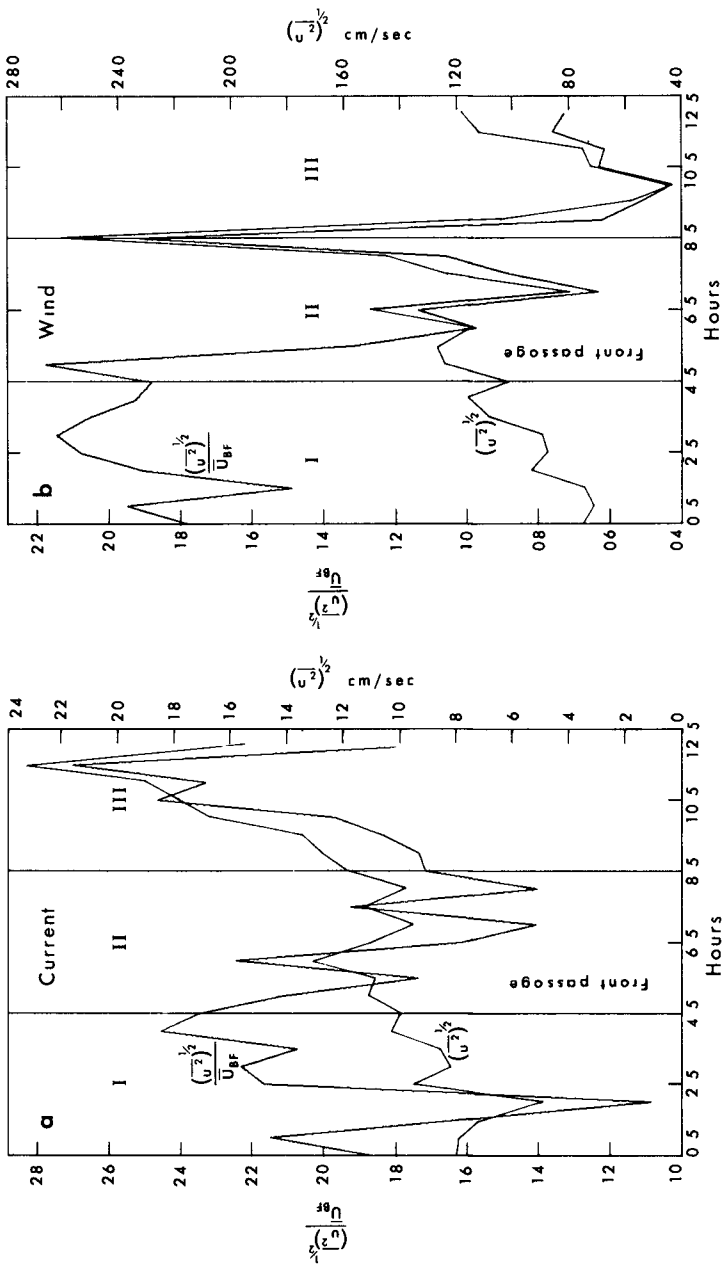

Fig 6 Turbulence intensity and relative turbulence intensity for (a) the current speed and (b) the wind speed

TURBULENCE SPECTRA

Energy density spectra F(f) of the two u' time series were calculated from the procedure outlined in Bendat and Piersol (1966, p 291) and modified by the use of a Fast Fourier Transform The 2400 data points were first divided into three segments (I, II, and III), as discussed earlier, each containing 800 points, so that the change of the energy density with the progress of the storm could be investigated The resulting current speed spectra are shown in Figure 7 In the frequency range 15 < f < 60 CPH there are no significant gaps or peaks apparent in any of the intervals, the energy density decreases smoothly with increasing frequency The apparent peak in spectrum II is not significant at the 0 05 level at f ≃ 50 CPH The peaks at about 12 CPH, of course, are a result of the low frequency cutoff by the filter As shown in Table 1, the total relative energy (the area under the spectral curve) more than quadruples from intervals I to III There is considerably more energy at all frequencies in successively higher intervals, but the greatest increase is clearly at the lowest frequencies Also listed in Table 1 is the absolute energy E associated with the turbulence in the mean flow direction, which is given by Taylor (1935) as

$$E = \frac{\rho}{2}\,\overline{(u'^2)}$$

The spectra in Figure 7 have also been corrected for the instrument frequency response R(f) plotted in Figure 2 The corrected spectral density F'(f), shown as a dashed line in Figure 7 and calculated from

$$F'(f) = \frac{F(f)}{R(f)^2},$$

has little effect other than to increase the energy at the high frequencies

The wind speed spectra in Figure 8 display the same lack of peaks or gaps as the current spectra Most notable is the fact that the energy content (see Table 1) does not increase at all from intervals II to III, in sharp contrast to the twofold increase observed in the content of the current spectra between these intervals This suggests again a lack of direct energy transfer between wind and current in the frequency band 10 < f < 60 CPH under study here This inference is

Table 1 Total Energy Associated with Energy Density Spectra

	RELATIVE $\int F(f)\,df$ $(cm/sec)^2$		ABSOLUTE E $(ergs/cm^3)$	
Interval	Current	Wind	Current	Wind
I	69	8281	34	4 1
II	119	15006	59	7 5
III	279	15126	139	7 6

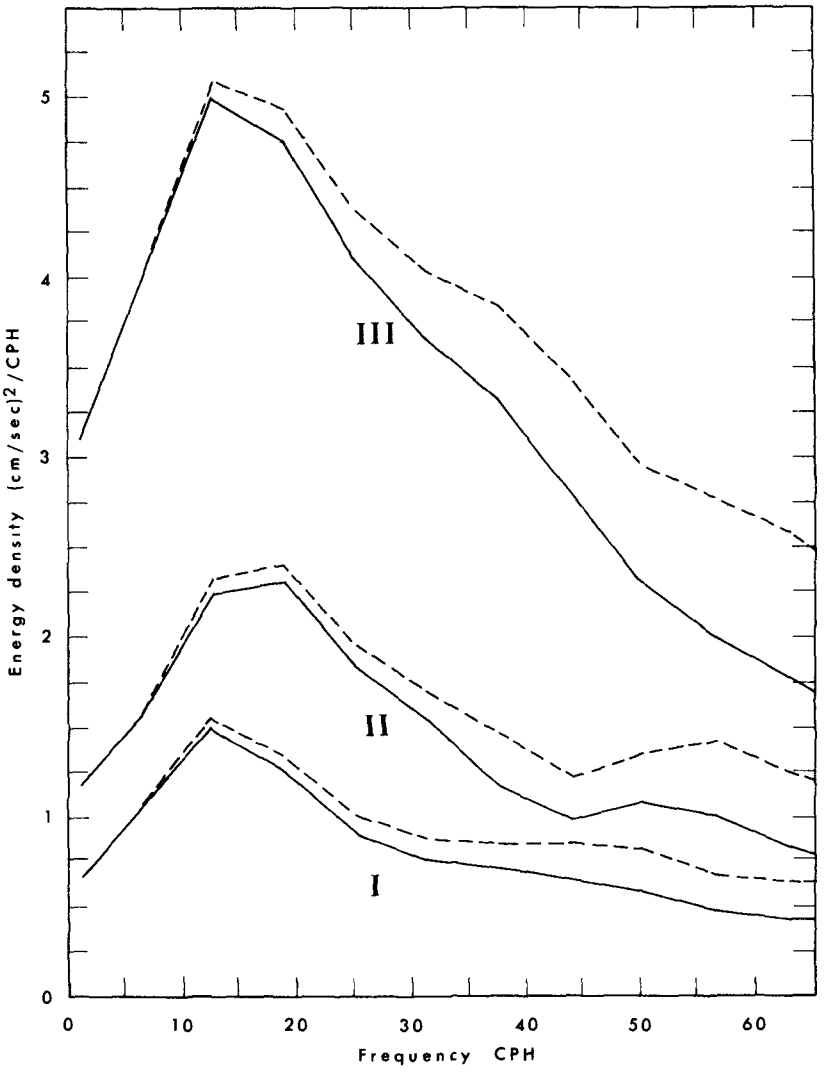

Fig 7 Energy density spectra of the current for the three phases of the storm The dashed line is a correction for the instrument frequency response

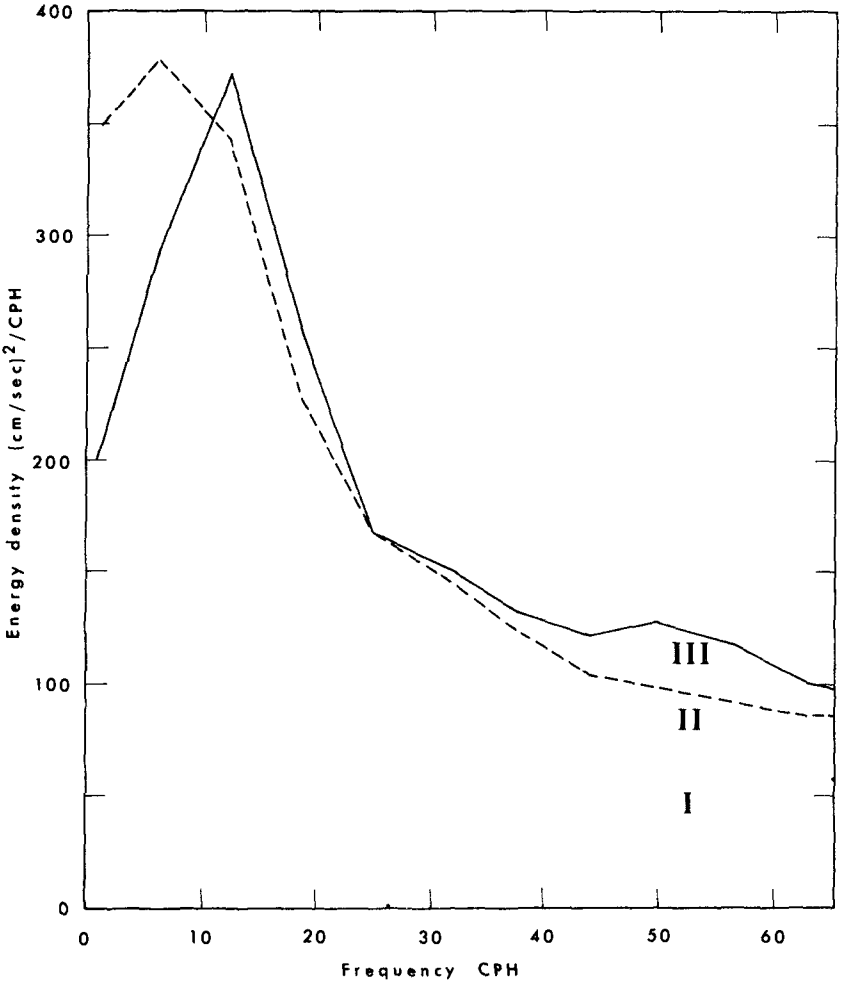

Fig 8 Energy density spectra of the wind speed for the three phases of the storm

supported by the data in Table 1, which shows that there are more ergs of energy per unit volume associated with the turbulence in the water than with that in the air at these frequencies

The data seem to indicate that the energy is entering the 10-60 CPH frequency band of the current from the lower frequency oscillations of the current itself, which are presumably generated by the low frequencies of the wind A good correlation does clearly exist between

the DC levels (mean values) of the wind and the current (see Fig 3 and Murray, 1970)

In Figure 9 the F(f) spectra of the wind are replotted on a log-log scale In studies of air turbulence over water Pond et al (1966) found that in the low frequency ranges of their data the energy density dropped off with the -1 power of the frequency $F(f) \propto f^{-1}$ Their -1 power range extended between $10^{-5} < k < 3 \times 10^{-3}$ where k is the wave number Using Taylor's hypothesis $f = Uk/2\pi$ (Taylor, 1938) and the limits of the mean values for this study $500 < U_{BF} < 1300$ cm/sec, the corresponding frequency band for their -1 power range is $3 < f < 2300$ CPH The present data which fall in the low frequency end of the range are also represented very well by the -1 power slope Tchen (1953) has suggested that the -1 power law would hold below the inertial sub-range

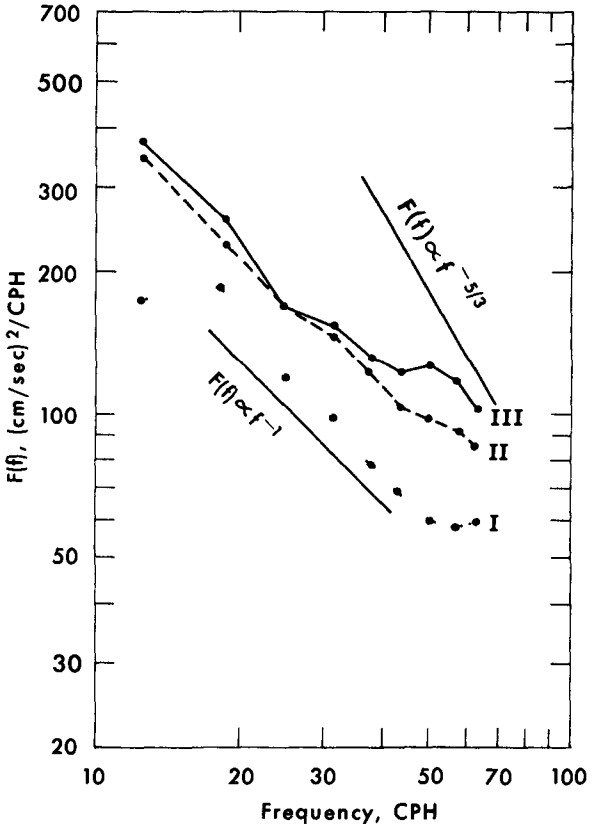

Fig 9 Energy density spectra of the wind on a log-log plot The straight lines show a -1 and a -5/3 power dependency on the frequency

in the presence of strong vertical shear--a situation which certainly existed in the lower 10 meters of the atmosphere during this storm as a result of surface drag

So that the energy drop-off with frequency of the F(f) spectra of the current speed may be similarly investigated, the spectra of Figure 7 are replotted on a log-log scale in Figure 10 Cannon (1969) has presented excellent and comprehensive data which clearly established the presence of a -5/3 law governing the drop-off of energy with frequency in an estuarine tidal flow in the frequency band $1 < f < 72$ CPH Cannon also reported, however, several experiments in which strong vertical shear was suspected and the log-log plots showed that $F(f) \propto f^{-1}$ During a large part of the 13-hour record used in this study the Q-16 meter was bounded by two shear zones (a) the bottom boundary layer and (b) the transition zone (probably near mid-depth) between upper-layer wind-driven

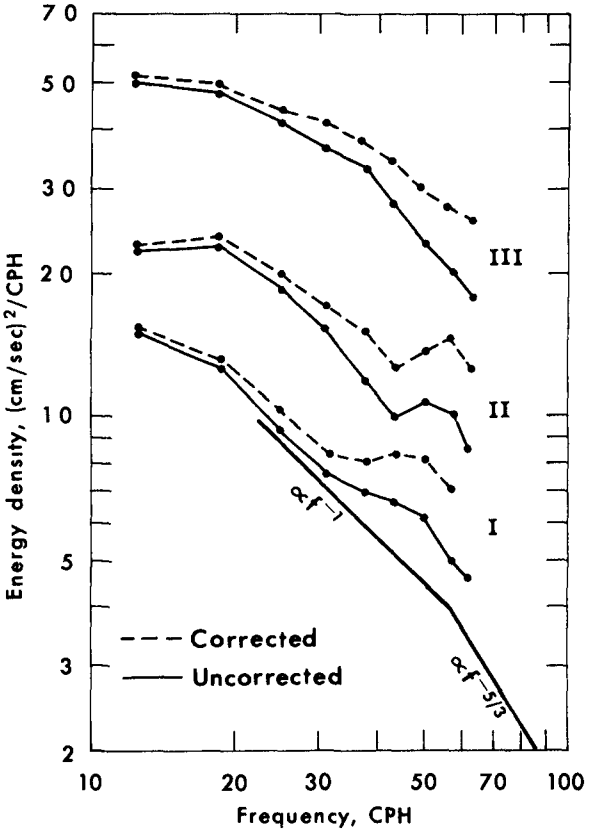

Fig 10 Energy density spectra of the current on a log-log plot The straight lines show a -1 and a -5/3 power dependency on the frequency

currents and lower-layer return flows caused by the setup against the coast (Murray, 1970) Figure 10 may reflect that this phenomenon as the -1 power is a reasonable fit for the spectra (both corrected and uncorrected) in intervals I and II However, in interval III of the current record, when the energy content was highest (Table 1), the slope of the spectra (on a log-log plot) was considerably flatter than the -1 value--having a value close to -0 5 These observations suggest that with increasing energy content (or perhaps increasing vertical shear) the F(f) dependency on the frequency may shift from $f^{-5/3}$ to f^{-1} to $\sim f^{-0\ 5}$ in this intermediate frequency range

CROSS CORRELATION

All attempts to relate the turbulent energy distribution in the wind to that of the current yielded negative results Figure 11 shows a typical wind-current coherence function (interval II), the coherence level is insignificant at all frequencies Similarly, the phase lags (Fig 12) from the same data set oscillate with no apparent pattern Such results are not unexpected since Cannon (1969), in carefully controlled experiments, found no significant coherence between the records of adjacent current meters in frequencies above 10 CPH

CONCLUDING REMARKS

The principal conclusions from this study of wind and water turbulence in the frequency band $10 < f < 60$ CPH are as follows

1 As the storm progresses there is no systematic change in the energy spectra common to both wind and current

2 As the storm progresses the energy content of the current spectra increases markedly, the maximum increase in energy is in the lowest frequencies

3 The coherence between wind and current is insignificant (< 1) in this band

4 For reasons 1, 2, and 3 above it is concluded that energy is fed into the 10-60 CPH frequency band of the current from the lower frequencies of the current itself

5 The energy density of the wind decreases proportionally to the -1 power of the frequency in all three storm intervals

6 The energy density of the current decreases proportionally to the -1 power of frequency in the first two intervals of the storm but proportionally to $\sim$0 5 power of the frequency during the third storm interval, which was the most intense

ACKNOWLEDGMENTS

Myron Young and Choule Sonu of Louisiana State University developed the programs which permitted this time series analysis to be carried out The project was sponsored by the Geography Programs, Office of Naval Research, under Contract N00014-69-A-0211-0003, NR 388 002

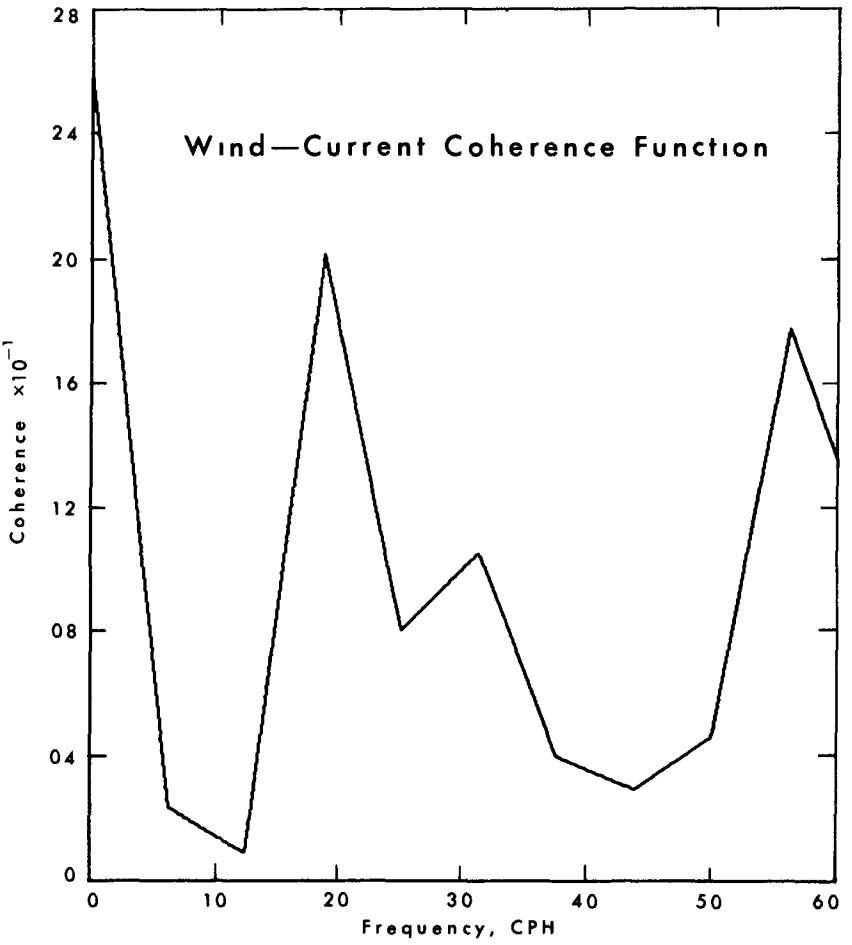

Fig 11 The coherence function between the wind and the current from interval II

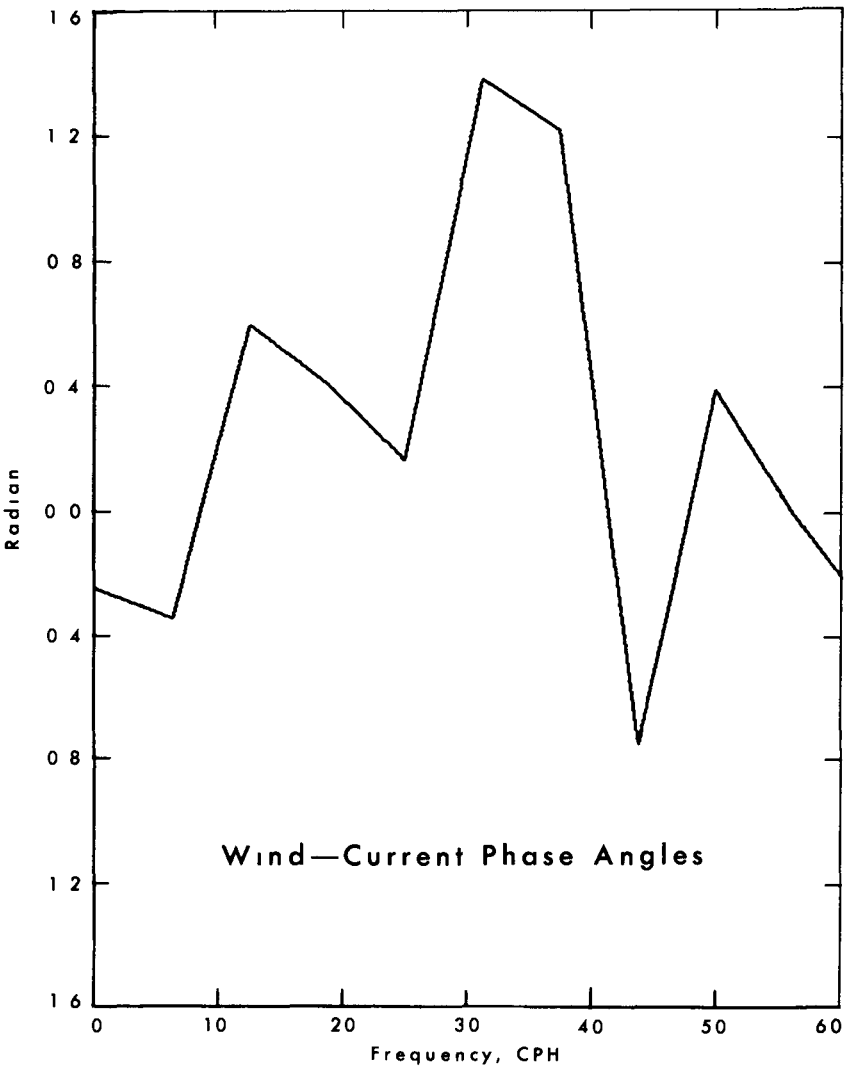

Fig 12 The phase lags of the wind and the current from interval II

REFERENCES

Bendat, J S , and A G Piersol, 1966, Measurement and analysis of random noise data New York (John Wiley), 390 pp

Cannon, G A , 1969, Observations of motion at intermediate and large scales in a coastal plain estuary Technical Report No 52, Ref 69-5, Chesapeake Bay Institute, The Johns Hopkins Univ , 113 pp

Fergusson, S P , 1935, The sensitiveness of anemometers Bull Am Meteorol Soc , 15 95-99

Holloway, J L , Jr , 1958, Smoothing and filtering of time series and space fields In (H E Landsberg, ed) Advances in geophysics, 4 351-388

Murray, S P , 1970, Bottom currents near the coast during Hurricane Camille J Geophys Res , 75(24) 4579-4582

Panofsky, H A , and G W Brier, 1963, Some applications of statistics to meteorology The Pennsylvania State Univ , University Park, Pennsylvania, 224 pp

Pond, S , S D Smith, P F Hamblin, and R W Burling, 1966, Spectra of velocity and temperature fluctuations in the atmospheric boundary layer over the sea J Atmospheric Sci, 23(4) 376-386

Taylor, G I , 1935, Statistical theory of turbulence Parts I-IV Proc Roy Soc London, A151, pp 421-478

_____, 1938, The spectrum of turbulence Proc Roy Soc London, A164, pp 476-479

Tchen, C M , 1953, On the spectrum of energy in turbulent shear flow J Res NBS, 50(51)